AGU PUBLICATIONS

Water Resources Research

RESEARCH ARTICLE
10.1002/2017WR021278

Influence of Slope-Scale Snowmelt on Catchment Response Simulated With the *Alpine3D* Model

Tristan Brauchli[1,2], Ernesto Trujillo[1,2], Hendrik Huwald[1], and Michael Lehning[1,2]

[1]School of Architecture, Civil and Environmental Engineering, Ecole Polytechnique Fédérale de Lausanne, Lausanne, Switzerland, [2]WSL Institute for Snow and Avalanche Research SLF, Davos Dorf, Switzerland

Key Points:
- Accurate representation of snow distribution is essential to reproduce differential snowmelt and runoff response in alpine catchments
- Precipitation interpolation remains a key element to estimate snow distribution
- Improved modeling of liquid water transport through the snowpack is critical at site-scale but with decreasing influence at larger scales

Supporting Information:
- Supporting Information S1

Correspondence to:
T. Brauchli,
tristan.brauchli@alumni.epfl.ch

Citation:
Brauchli, T., Trujillo, E., Huwald, H., & Lehning, M. (2017). Influence of slope-scale snowmelt on catchment response simulated with the *Alpine3D* model. *Water Resources Research*, *53*, 10,723–10,739. https://doi.org/10.1002/2017WR021278

Received 8 JUN 2017
Accepted 5 DEC 2017
Accepted article online 7 DEC 2017
Published online 21 DEC 2017

Abstract Snow and hydrological modeling in alpine environments remains challenging because of the complexity of the processes affecting the mass and energy balance. This study examines the influence of snowmelt on the hydrological response of a high-alpine catchment of 43.2 km^2 in the Swiss Alps during the water year 2014–2015. Based on recent advances in *Alpine3D*, we examine how snow distributions and liquid water transport within the snowpack influence runoff dynamics. By combining these results with multiscale observations (snow lysimeter, distributed snow depths, and streamflow), we demonstrate the added value of a more realistic snow distribution at the onset of melt season. At the site scale, snowpack runoff is well simulated when the mass balance errors are corrected ($R^2 = 0.95$ versus $R^2 = 0.61$). At the subbasin scale, a more heterogeneous snowpack leads to a more rapid runoff pulse originating in the shallower areas while an extended melting period (by a month) is caused by snowmelt from deeper areas. This is a marked improvement over results obtained using a traditional precipitation interpolation method. Hydrological response is also improved by the more realistic snowpack (NSE of 0.85 versus 0.74), even though calibration processes smoothen out the differences. The added value of a more complex liquid water transport scheme is obvious at the site scale but decreases at larger scales. Our results highlight not only the importance but also the difficulty of getting a realistic snowpack distribution even in a well-instrumented area and present a model validation from multiscale experimental data sets.

1. Introduction

Snow is an essential component of the hydrologic cycle of mountain regions across the globe (Beniston, 1997; Serreze et al., 1999). Mountain snowpacks are a major water resource for regional ecosystems, groundwater recharge, human consumption, agriculture, and hydropower, among others. The hydrology of mountain regions is expected to be strongly affected by climate change (Barnett et al., 2005; Stewart, 2009), with shorter snow seasons and reduced snowpack storage (Bavay et al., 2009; Burn, 1994; Horton et al., 2006) and slower melt as a result of earlier snowmelt seasons (Marty et al., 2017; Musselman et al., 2017). These changes in snow regimes can have a negative impact for hydropower production (Schaefli et al., 2007), winter sports (Schmucki et al., 2017; Scott et al., 2008) and mountain forests (Bales et al., 2011; Trujillo et al., 2012; Westerling, 2006), evapotranspiration, and carbon uptake (Winchell et al., 2016).

Accurate snowpack modeling is paramount to properly understand how these expected changes in climate affect snowpack processes in mountain regions (Bales et al., 2006; Viviroli et al., 2011). However, significant challenges in snow modeling still exist because of the complexity of snow processes across multiple scales (Blöschl, 1999; Clark et al., 2011). Snow accumulation and melt are highly variable in space and time and are difficult to represent in snow models (Dozier, 2011). Precipitation is very heterogeneous featuring complex patterns both at regional and watershed scales (Roe, 2005; Scipión et al., 2013; Sevruk, 1997; Sommer et al., 2015). Wind, topography, and vegetation control deposition and redistribution of snow, impacting the distribution patterns across scales (Grünewald et al., 2014; Lehning et al., 2008; Mott et al., 2014; Schirmer et al., 2011; Trujillo et al., 2007, 2009). Following deposition, snow distribution is affected by avalanching and sloughing (Blöschl & Kirnbauer, 1992), radiation processes controlled by seasonal changes in temperature, solar radiation, cloud cover, topographic shading, and snow radiative properties (Lehning, 2006; Marks & Dozier, 1992). Vegetation influences the mass and energy balance by modifying the micrometeorological conditions and changing the radiative fluxes (Harding & Pomeroy, 1996). All these processes lead to highly heterogeneous snow distribution and snow physical properties. As a result, energy balance and snowmelt

processes are also heterogeneous in space. This heterogeneity is accentuated later in the snowmelt season by the patchy nature of the snow cover modifying radiative and turbulent heat fluxes, and ultimately snow melt (Grünewald et al., 2010; Mott et al., 2013). The hydrological response is then no longer proportional to the direct mass input from the atmosphere but rather to the combination of locally accumulated mass and the site specific energy balance (Lundquist & Dettinger, 2005; Woo, 2006).

Physically based snow models (e.g., *Crocus* (Brun et al., 1989), *Isnobal* (Marks et al., 1999), and *SNOWPACK* (Lehning et al., 1999)) have become increasingly popular due to the availability of higher quality and higher (spatial) density of required meteorological input, and improvements in modeling and numerical methods. Better validation through recent snow measuring techniques and remote sensing technologies has also increased acceptance of more complicated models (e.g., Wever et al., 2017). While computationally intensive and often more vulnerable to data quality issues (Schlögl et al., 2016), these models require reduced parameter calibration and are expected to be more reliable when extrapolated to different conditions (e.g., climate change scenarios) or interpolated spatially over a larger region (Essery et al., 2009; Etchevers et al., 2004). However, complexity increases along with the necessity to accurately model some of the detailed processes involved at the range of scales over which the processes take place (Blöschl, 1999). The spatial resolution will define which processes are explicitly resolved and which ones are parameterized or simply not represented (Clark et al., 2011). In many cases, the computing power still remains a limiting factor.

In the present study, we assess the impact of recent developments in the physically based *Alpine3D* model (Lehning et al., 2006) on snowpack simulation and its melt. The objective of this study is to analyze the ability of *Alpine3D* to reproduce the snow cover evolution across multiple scales. Two recent advances are of particular interest for studying the hydrological response. First, Wever et al. (2014) implemented the Richards equation to model the liquid water transport in the snow cover. Second, Vögeli et al. (2016) proposed a new methodology that assimilates snow depth measurements in the precipitation interpolation scheme. We assess the impact of these new schemes by comparing model output to different experimental field data. In particular, we carry out detailed multiscale (plot, subcatchment/hillslope, and catchment) analyses of heterogeneity in snow cover and snowmelt patterns and their consequences on timing and magnitude of streamflow. The study focuses on spatial scales relevant for the accurate representation of the hydrological response of a complex high-alpine headwater catchment, the Dischma River basin in Switzerland (Figure 1), during the water year 2014–2015. Two components of the modeling system are

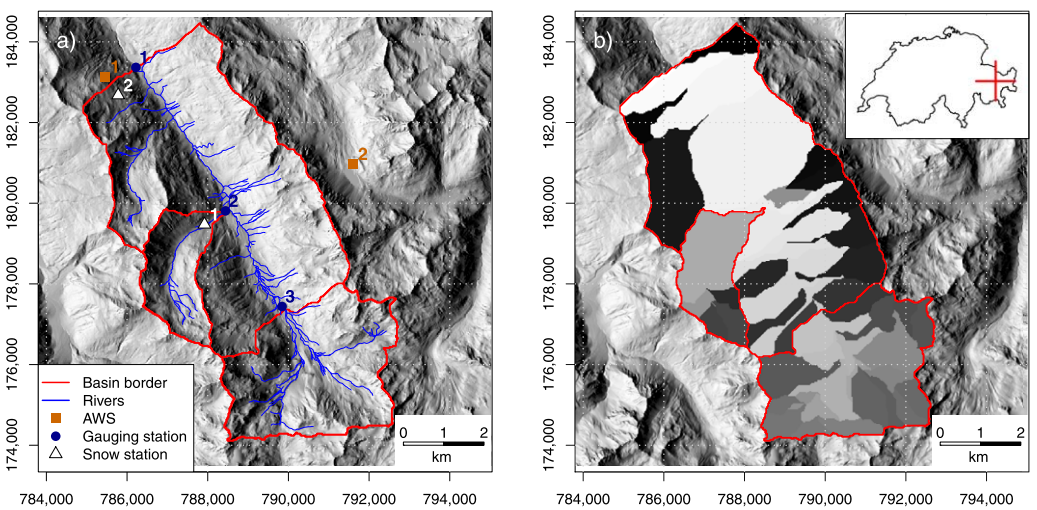

Figure 1. (a) The Dischma River basin and the two monitored subcatchments are delineated in red with their outlet in dark blue: (1) Kriegsmatte, (2) Am Rin, and (3) Duerrboden. White triangles indicate the snowmelt lysimeter stations: (1) the Rinertaelli site and (2) the Stillberg site. Automatic weather stations are marked with orange squares: (1) the Stillberg *IMIS* station and (2) the Fluelapass *IMIS* station. The river network is shown in blue. (b) The Dischma River basin divided into 55 subbasins for hydrological modeling. Reproduced with permission from *swisstopo* (JA110138).

instrumental for the analysis: (1) *Alpine3D*, the spatially distributed version of *SNOWPACK*, enables a detailed representation of the atmosphere-vegetation-soil continuum. It has been extensively used for studying the snow cover evolution (Comola et al., 2015; Schmucki et al., 2014), its sensitivity to climate change (Bavay et al., 2009, 2013), snow transport (Mott et al., 2010), and glacier hydrology (Michlmayr et al., 2008). (2) The *StreamFlow* model (Gallice et al., 2016), which coupled to *Alpine3D*, enables simulation of hydrological response at the catchment scale.

2. Study Area

The Dischma River basin (Figure 1) covers an area of 43.2 km^2 with an elevation range between 1,668 and 3,146 m (mean: 2,372 m). The basin has a SE-NW orientation, with two dominating hillslopes facing northeast and southwest, respectively. The headwaters of the catchment form a north-facing bowl with a small glacier (0.9 km^2, 2.1% of the contributing area) at the highest elevations. On the southwest side of the main valley, there are two small subwatersheds with north- and south-facing slopes. The land cover is representative of the alpine region: 36% of the valley is covered by subalpine meadows; bare soil and exposed bedrock cover about 50% of the basin; forest and shrubs less than 10%. On the hillslopes, soils (mainly Orthents, Rankers, and Entisols) are relatively shallow ($<$0.50 m on average), highly permeable (mean hydraulic conductivity: 4.3×10^{-4} m s^{-1}), and with limited water retention capacity (mean: 17.8 mm; FOEN, 2017). Deeper soils (Fluvents) are found along the valley bottom with a more significant groundwater storage (Gurtz et al., 2003). The geological bedrock is mainly composed of crystalline rocks (orthogneiss, paragneiss, and amphibolites; Verbunt et al., 2003).

From a climatological point of view, the Dischma catchment is located at the border between the wetter northern flank of the Alps and the drier inner-alpine area (Frei & Schär, 1998). Due to its position, the basin is rather sheltered and receives below-average precipitation (mean annual precipitation in Switzerland (1961–1990): 1,458 mm; Spreafico & Weingartner, 2005). The mean annual precipitation in Davos (located at 1,594 m and 5 km northward) over the period 1974–2015 amounts to 1,039 mm yr^{-1}. At "Kesch" hut, located at 2,570 m southwest of the Dischma basin, the average annual precipitation is 1,251 mm yr^{-1} over the same period. The resulting altitudinal gradient of 22 mm/100 m (or 2%/100 m) is small for the alpine region but in agreement with corresponding values in the literature (Sevruk, 1997). Finally, evapotranspiration is moderate ($\sim$250 mm yr^{-1}; Menzel et al., 1999).

The hydrological regime is glacio-nival (Aschwanden et al., 1985) with low flows during winter and high flows in springtime and summer due to snow and ice melt. During this period, the diurnal variation in energy input mainly controls the magnitude and timing of the discharge. The mean annual discharge over the period 1961–1980 was 1,245 mm yr^{-1} (Schädler & Weingartner, 1992).

3. Data

3.1. Snow Lysimeter

Snow lysimeters were deployed to quantify water output at the base of the snowpack and to detect the onset of the melting season. This type of instrumentation has been used in multiple snow studies to measure runoff from snowmelt (Kinar & Pomeroy 2015). Permanent instrumentation generally have larger collecting areas to increase data representativeness (Kattelmann, 2000), which is especially important for heavily stratified and heterogeneous snowpacks. For this study, nonpermanent instruments of smaller size (0.45 m of diameter) were deployed with a setup similar to Würzer et al. (2016). Instrument sites are indicated in Figure 1a: (a) on a south-facing slope in the "Rinertaelli" side-valley and (b) on a northeast-facing slope close to the "Stillberg" weather station. The two sites are chosen at a similar elevation in order to facilitate direct comparison: differences in snow accumulation and melt are mainly influenced by aspect and topography.

3.2. Discharge Data

The Swiss Federal Office for the Environment is monitoring discharge from the Dischma River catchment at the "Kriegsmatte" outlet (blue circle in Figure 1a), which is considered the reference discharge of the watershed. Two additional gauging stations were installed in early 2015 at upstream locations with the aim of capturing the hydrological response of subwatersheds with different geomorphological characteristics. The

first station, "Am Rin," is located on a lateral tributary just before its confluence with the main stream (Figure 1a). The side-valley "Rinertaelli" covers an area of 4.3 km^2 (10% of the entire basin) and has southeast-facing and north-facing slopes. The second gauging station is "Duerrboden" on the main stream monitoring the headwaters of the Dischma River. This subwatershed is composed of a large cirque facing north and covering 12.1 km^2 (28% of the basin). Discharge was estimated using the salt dilution method (Day, 1976). A rating curve for each site was derived allowing for the transformation of water depth into discharge following Weijs et al. (2013).

3.3. Meteorological Data

For the chosen configuration (detailed in section 4), *Alpine3D* requires the meteorological variables listed in Table 1. Two networks are used to complement the required data in the Dischma catchment area:

a. The Swiss Federal Office of Meteorology, *MeteoSwiss*, operates an automatic weather station (AWS) network covering the entire country. In the Dischma area, two stations are used: (i) "Davos" (DAV) and (ii) "Weissfluhjoch" (WFJ) on the mountain range northward of Davos. Data analysis of the precipitation time series (1974–2015) revealed that the WFJ rain gauge recorded consistently more precipitation than the storage precipitation gauge in "Kesch" hut (1,359 mm yr^{-1} at WFJ versus 1,251 mm yr^{-1}, $\Delta P = 108$ mm or 9%) located at similar elevation 20 km southward. These differences can be explained by the north-south precipitation gradient discussed in section 2. Therefore, we only used precipitation amounts from the "Davos" station and applied an altitudinal gradient estimated from the difference between the DAV station and the "Kesch" hut.
b. The Inter-cantonal Measurement and Information System (*IMIS*) is a network of AWS covering high-altitude areas (2,500–3,500 m) in Switzerland (Lehning et al., 1999). As a result of limited power supply, *IMIS* station sensors are not heated or ventilated. The stations located around the Dischma catchment are listed in Table 1, two of them are shown in Figure 1a. It is worth noting that these snow depth measurements are only used for validation purposes.

3.4. Snow Depth Map

Digital surface models (DSM) were derived from stereo imaging captured by airborne digital sensors (ADS; Bühler et al., 2015). Two flights covering the Dischma basin were carried out, one during summer (3 September 2013) and one close to peak accumulation (15 April 2015). The snow depth data set is obtained by subtracting the summer DSM from the winter surface. The spatial resolution is 2 m and its accuracy ±30 cm (Bühler et al., 2015). The data set contains spatial gaps because of the limitations of ADS to measure snow height over buildings, vegetated areas, and water bodies. The data were then averaged over 100 m grid cells to match the *Alpine3D* grid. A minimum of 50% of valid data coverage was set as a threshold (similar to Vögeli et al., 2016) to ensure consistency in the aggregated snow depths. This data set is used for validation of the modeled snow cover and is assimilated as a correction factor in the precipitation interpolation (section 4.1).

Table 1
Automatic Weather Stations (AWS), Position (Easting/Northing in Geodetic Datum CH1903), and Measured Meteorological Variables (TA, Air Temperature; RH, Relative Humidity; WV, Wind Speed; ISWR, Incoming Shortwave Radiation; ILWR, Incoming Longwave Radiation; P: Precipitation; HS: Snow Depth) Part of the MeteoSwiss *(MCH) and* IMIS *Networks*

Station name/type	Position (m)	Altitude (m)	TA	RH	WV	ISWR	ILWR	P	HS
Weissfluhjoch (*MCH* + *IMIS*)	780,853/189,229	2,540	×	×	×	×	×	+	V
Davos (*MCH*)	783,514/187,457	1,594	×	×	×	×	×	×	V
Davos-SLF (*IMIS*)	783,800/187,400	1,560	×	+	×	−	−	−	V
Stillberg (*IMIS*)	785,455/183,136	2,085	×	×	×	×	×	+	V
Puelschezza (*IMIS*)	797,300/175,080	2,680	×	×	×	−	−	−	V
Fluelapass (*IMIS*)	791,600/180,975	2,390	×	×	×	−	−	−	V
Baerentaelli (*IMIS*)	782,100/174,760	2,560	×	×	×	−	−	−	V

Note. Variables marked with an "×" are measured at that station and used in the modeling process. Notation "V" means used for validation purposes only. The "+" are measured but not used in the modeling. The "−" signs indicate variables that are not measured at the weather station.

4. Models and Methods

4.1. *Alpine3D* Setup

The one-dimensional *SNOWPACK* model (Lehning et al., 1999) computes the energy and mass balance of a multilayer snowpack and its underlying soil layers. Its spatially distributed version, *Alpine3D*, runs the same algorithm on a regular mesh grid without considering lateral exchange in the soil-snow-vegetation column. The model is run at a 15 min time step with a grid cell size of 100 m over a domain of 154 by 128 elements. The Dischma area is represented in terms of topography and land use by incorporating the digital elevation model and soil properties provided by the Federal Office of Topography. The turbulent heat fluxes are simulated based on Monin Obukhov (MO) similarity theory and stability corrections as described by Michlmayr et al. (2008). The roughness length of the snow cover is set to 0.007 m. Vegetation influence is simulated with a two-layer canopy model developed for evergreen coniferous forests (Gouttevin et al., 2015).

Interpolation of meteorological forcing data is carried out using *meteoIO* (Bavay & Egger, 2014). This module contains routines for spatiotemporal interpolation and filtering of erroneous data. This study uses the following model setup:

1. For precipitation, data from *MeteoSwiss* station DAV are corrected for precipitation undercatch (Goodison et al., 1997). Spatial interpolation is performed by applying a fractional lapse rate of 2%/100 m (see section 2). The precipitation phase is determined based on an air temperature threshold of +1.5°C; above this value all precipitation is considered liquid. The hillslope-scale snow variability is modeled by assimilating snow depth data in the precipitation interpolation scheme (Vögeli et al., 2016). This method consists in applying a spatial correction factor to the precipitation field based on observed snow depth fields. This results in a more realistic snow height distribution while conserving the mass balance over the entire catchment. In practice, precipitation $P_{i,t}$ at a given grid point i and at time t is computed as follows:

$$P_{i,t} = \frac{HS_i}{HS_{avg}} \times P_{avg,t}$$

   where $P_{avg,t}$ is the average interpolated precipitation over the basin at time t, HS_i the measured snow depth at the given grid point i, and HS_{avg} is the mean ADS snow depth over the catchment. Note that we could not run the snow transport module of *Alpine3D*, which is computationally too demanding for the size of the area but would significantly increase the heterogeneity of snow (Mott & Lehning, 2010).
2. For the incoming shortwave radiation (ISWR), the atmospheric attenuation coefficient and direct/diffuse radiation apportionments are computed for each station separately as a function of the local potential maximum solar radiation. These values are then interpolated over the grid using inverse distance weighting (IDW) and taking into account topographic shading.
3. All other meteorological variables are interpolated applying IDW and an altitude-dependent lapse rate (Bavay & Egger, 2014).

Liquid water transport in the snow cover and in the soil layer is simulated either by a simple bucket approach or using the Richards equation (RE; Wever et al., 2014). In the first approach, the liquid water content of a layer is constrained by an upper threshold; once this water holding capacity is exceeded, water is drained down to the next layer. The water holding capacity is a direct function of the volumetric ice/soil content (Wever et al., 2014). The second method relies on the Richards equation originally developed for water movement in unsaturated soils and recently implemented for the vertical water movement in snow by Wever et al. (2014). This implementation relies on the Van Genuchten (1980) water retention model and the parameterization proposed by Yamaguchi et al. (2012).

For comparison *Alpine3D* is run in four different configurations:

1. *Reference* + *Bucket scheme* (*Ref-BK*). Precipitation is interpolated based on measurements from the Davos station plus a fractional lapse rate of 2%/100 m. Liquid water transport in the snowpack is simulated following the bucket approach.
2. *Scaling* + *Bucket scheme* (*Scal-BK*). Precipitation is scaled following the method of Vögeli et al. (2016) as described above. Liquid water transport in the snowpack is based on the bucket approach.

3. *Reference + Richards equation* (*Ref-RE*). Precipitation is interpolated based on measurements from the Davos station plus an altitudinal gradient of 2%/100 m. Liquid water transport in the snowpack is simulated using the Richards equation.
4. *Scaling + Richards equation* (*Scal-RE*). Precipitation is scaled following the method of Vögeli et al. (2016). Liquid water transport in the snowpack is simulated using the Richards equation.

4.2. *StreamFlow* Setup

StreamFlow (Gallice et al., 2016) is the hydrological extension of *Alpine3D*. This spatially explicit model relies on the travel time distribution (Botter et al., 2010; Comola et al., 2015) of water particles in a subcatchment. For each subcatchment, the mass balance is described by two superimposed linear reservoirs mimicking the fast and slow subsurface runoff, respectively. The lower bucket is supplied by the soil runoff originating from *Alpine3D* up to a maximum recharge rate R_{max} (m s^{-1}) while the upper reservoir collects the excess water. The runoff generation itself is controlled by the mean travel time $\tau_{res,u}$ and $\tau_{res,l}$ (s) of water particles in each reservoir. The subwatershed runoff is then injected into the stream network and routed to the outlet. Using the TauDEM algorithm (Tarboton, 1997), the Dischma basin was divided into 55 subwatersheds with a mean area of 0.79 km^2 and its stream network was delineated (Figure 1b). For the calibration, we opted for a Monte-Carlo approach and chose the best parameter values for R_{max}, $\tau_{res,u}$, and $\tau_{res,l}$ by optimizing the Nash-Sutcliffe model efficiency (NSE) coefficient (Nash & Sutcliffe, 1970) independently for each of the four model configurations. With this individual calibration, the differences in model results highlight the influence of water input on the hydrological response and we avoid biases induced by suboptimal parameter sets. The calibration is carried out on measured discharge at the Dischma basin outlet only. Observations from the subbasins are used for validation purposes. The streamflow seasonality is evaluated through the centroid in time (CT) of the daily discharge proposed by Stewart et al. (2005). Finally, the results presented below are the average of the 100 best simulations for each model configuration in order to have a more robust signal.

5. Results

5.1. Snow Depths at Peak Accumulation

In high-altitude alpine catchments, snow cover at peak accumulation can be considered as the initial condition of the system for the spring melting season. The results of the reference simulation (Ref-BK) fail to reproduce the observed snow depth distribution patterns (Figure 2a, $R^2 = 0.34$) with most of the modeled values between 1 and 2 m. Shallow snow depths are largely overestimated, especially on south-facing slopes (green range in the color scale in Figure 2a), while the deeper snow depths are largely underestimated. Simulated snow depths barely reach values larger than 2 m, whereas observations can reach up to 3.5–4 m. The scaling approach (Scal-BK) brings the distribution of modeled snow depths much closer to the observed values (Figure 2b). The range is also wider with values between 0 and 4 m, and the scatter around the 1:1 line is significantly reduced ($R^2 = 0.96$). The root-mean-squared error is only 0.27 m compared to 0.62 m for the Ref-BK simulation. The scaling method shows a small positive bias (mean absolute error [MAE] = 0.25 m) for values between 0.5 and 4 m. During this period, a strong settling or compaction of the snowpack was observed over the entire basin, which could partially explain these differences (supporting information Figure S1, see also extensive discussion in Vögeli et al. (2016)). On the other hand, the Scal-BK simulation results slightly underestimate snow depth values below 0.5 m (MAE = 0.12 m). The ADS snow depths were obtained around peak accumulation, but some low-elevation parts or south-facing slopes of the basin had already experienced limited melt. *Alpine3D* assimilates the data set, inherently containing this bias, but the model computes the melting and settling processes again. This leads to an overestimation of these two phenomena (i.e., melt and settling) and consequently leads to an underestimation of the snow thickness (especially at lower elevations). These results are similar to the findings of Vögeli et al. (2016) for the winters of 2011/2012, 2012/2013, and 2013/2014.

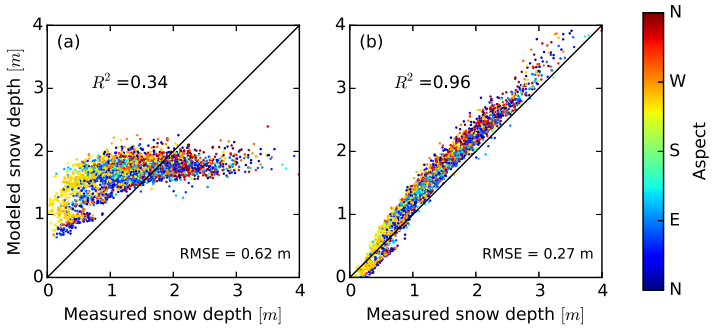

Figure 2. Modeled versus measured (ADS) snow depths over the Dischma River basin on 15 April 2015 (around peak accumulation). (a) Reference simulation (Ref-BK) and (b) the scaling method (Scal-BK). Color indicates the aspect of each grid cell.

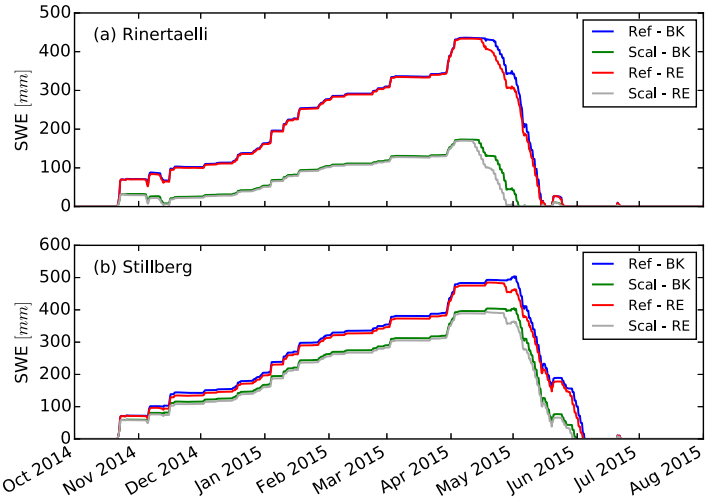

Figure 3. Comparison of modeled SWE at (a) the Rinertaelli and (b) the Stillberg sites for the four configurations: (1) reference interpolation and bucket scheme (Ref-BK), (2) scaling method and bucket scheme (Scal-BK), (3) reference interpolation and Richards equation (Ref-RE), and (4) scaling method and Richards equation (Scal-RE).

The peak accumulation snow variability is also a good indicator of which part of the natural processes the model is able to reproduce. As expected, the scaling approach is performing much better (snow depth coefficient of variation (CV) = 0.46–0.48 compared to 0.5 for the ADS data) than the reference scheme (CV = 0.20–0.21). More interestingly, the original ADS data at 2 m resolution have a CV of 0.7, which is likely still smaller than the true spatial variability of the snowpack. At the chosen resolution, the snow variability in the model is significantly filtered out. Detailed statistics are presented in supporting information Table S1.

5.2. Site-Scale Comparison of Snow Accumulation and Melt

The temporal snowpack evolution at Rinertaelli (SE facing) and Stillberg (NE facing) highlights the deficiency of the reference precipitation interpolation scheme for reproducing the snowpack spatial heterogeneity (Figure 3 and supporting information Figure S1 for a comparison with measurements). Even though the two sites have opposite aspects, their evolution throughout the winter is relatively similar, which should not be the case (due to melt events at the beginning of the winter and the local energy balance leading to enhanced settling at southerly expositions). At the end of the accumulation season, the difference in snow water equivalent (SWE) is only about 10%. During the ablation period, the heterogeneity of melt patterns between the two sites (as a consequence of differences in the local energy balance) seems well captured by *Alpine3D* with a much faster disappearance of snow on the south-facing slope (20 days earlier).

At Rinertaelli, the precipitation scaling sharply reduces snow accumulation, reaching only 40% SWE at the maximum compared to the reference simulation, and is much closer to observations (∼45 cm in the ADS data set versus ∼40 cm in the model, supporting information Figure S1a). Shallower snowpacks require less energy to reach isothermal conditions, and melting starts 3–4 days earlier (14 April versus 17 April with the BK scheme and 11 April versus 15 April with RE scheme). The combination of these two factors results in a shorter snow cover duration and the site becomes snow free 11–12 days earlier than in the reference simulation depending on the liquid water transport scheme.

At the Stillberg site, the impact of the precipitation scaling method is smaller. At peak accumulation (20 April 2015), SWE is only 18% lower than in the reference simulation. Compared to Rinertaelli, this difference is not large enough to notably change the thermal state of the snowpack (not shown) but still reduces the snow duration by 4 days. When validating the model output with the snow depth measured at the Stillberg meteorological station (located 500 m away from our site, and at similar elevation), the scaling approach leads to improved results in snowpack evolution, melt dynamics and snow disappearance date (supporting information Figure S1b). The above two examples show how increased snow depth variability results in larger spatial heterogeneity in melt dynamics, and in consequence, in melt-out dates.

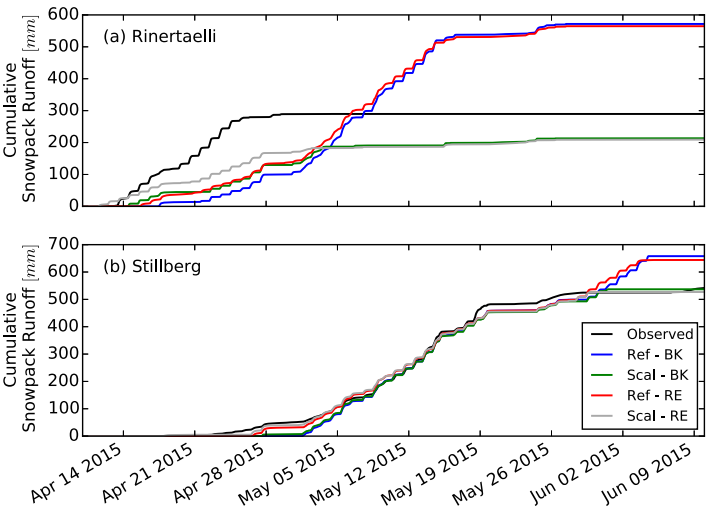

Figure 4. Cumulative liquid water output at the base of the snowpack at (a) Rinertaelli and (b) Stillberg for the four model configurations.

When using the Richards equation, melt water is routed faster through the snowpack that becomes isothermal earlier (not shown). Thus, liquid water is released at the base of the snowpack a few days earlier than for the bucket scheme. This effect is visible at both sites, although the difference in water release between the two schemes is more pronounced at the shallower Rinertaelli site (Figure 3a). These observations are in agreement with the results of Wever et al. (2015), who found a change of the snow internal energy budget with the Richards equation.

Table 2
Nash-Sutcliffe Efficiency Coefficient (NSE) and Coefficient of Determination (R^2) of the Liquid Water Output and Its Cumulative Value in Rinertaelli and Stillberg for the Four Different Model Configurations

		Liquid output		Cumulative liquid output	
		NSE	R^2	NSE	R^2
Rinertaelli	Ref-BK	−1.67	0.00	−1.96	0.56
	Scal-BK	−0.05	0.10	0.32	0.85
	Ref-RE	−1.36	0.00	−1.69	0.61
	Scal-RE	0.23	0.25	0.45	0.95
Stillberg	Ref-BK	−0.14	0.40	0.95	0.97
	Scal-BK	0.36	0.55	0.99	0.99
	Ref-RE	0.16	0.44	0.96	0.98
	Scal-RE	0.59	0.66	0.99	0.99

The two lysimeters enable an original comparison of snowpack liquid water output at the site scale with model output. On the southeast-facing slope (Figure 4a), the shallow snowpack produces rapid outflow following mid-April. The scaling approach combined with the Richards equation performs really well with respect to timing: the melt season starts on 11 April, 1 day earlier compared to the observations. The reproduction of daily cycles is satisfactory (Table 2, $NSE_{Scal\text{-}RE} = 0.234$), although the intensities are underestimated (Figure 5a). Simulated snowpack runoff increases rapidly in the morning and reaches a maximum in the early afternoon, slightly delayed compared to measurements. The subsequent recession limb approaches zero around midnight. Observed outflow never entirely reaches 0. When classic interpolation is used in combination with the Richards equation, the runoff peak is delayed due to longer travel times through the deeper snowpack while dynamics remain similar ($NSE_{Ref\text{-}RE} = -1.356$). The signal resulting from the bucket scheme is less accurate: timing and magnitude are satisfactory but the threshold effect prevents accurate reproduction of the recession curve ($NSE_{Ref\text{-}BK} = -1.67$, $NSE_{Scal\text{-}BK} = -0.05$). Also this observation is consistent with the results from Wever et al. (2014), who showed that the RE scheme clearly outperforms the bucket scheme at subdaily time scales. When looking at the slopes of cumulative runoff for the Rinertaelli site (Figure 4a), no simulation is able to reproduce the observed output rates leading to an noticeable discrepancy at the end of the melt season. In terms of mass balance, the reference interpolation scheme overestimates the cumulative outflow by about a factor of 2 while the scaling approach is much closer to the observations (30% underestimation). These results corroborate the negative bias noticed above for shallow snowpack at peak accumulation.

At the Stillberg site (NE facing), melt dynamics are different than at Rinertaelli (Figure 4a versus Figure 4b). Snowmelt starts on 18 April, 6 days later than at Rinertaelli, and produces very limited outflow during the first 3 days. The deeper snowpack holds a nonnegligible part of the liquid water in the snow matrix during that period. Starting on 21 April, runoff slightly increases. None of the model configurations is able to reproduce the onset of the melt season perfectly; however, simulations using the Richards equation are closer to the observed onset and produce larger melt rates than with the bucket scheme. Snowmelt sharply increases at the beginning of May when the snowpack at Rinertaelli has already disappeared. The daily cycle, notably the timing, is very well captured in the model configurations using the Richards equation (Figure 5b, $NSE_{Scal\text{-}RE} = 0.593$). These simulations reproduce the recession curve very well and even sustain an outflow during nighttime. Contrary to the south-facing site, the maximum intensities are slightly larger than observed. The scaling approach compensates for the total volume error by slightly reducing the total precipitation. Discrepancies between the observed and modeled cumulative runoff are very minor (Figure 4b) indicating correct representation of melt dynamics. Note that ISWR and ILWR are measured at the Stillberg weather station and both are used in the modeling calculations. Thus, interpolation errors for these quantities are small due to the vicinity of the station to the snow site.

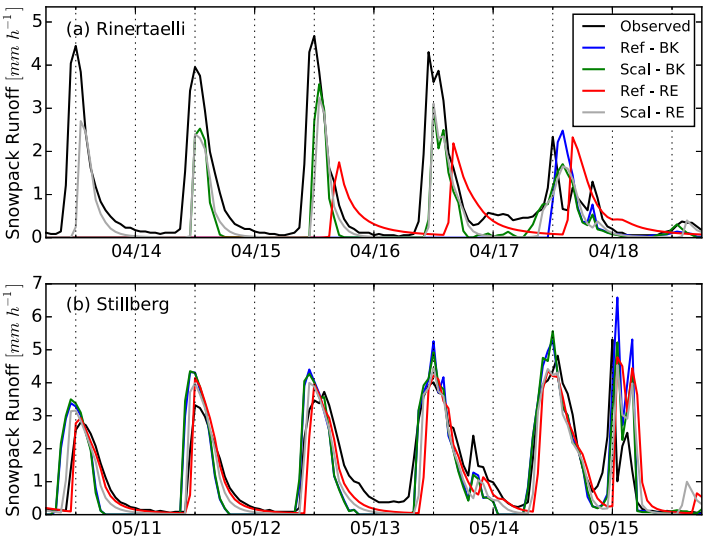

Figure 5. Comparison of observed and simulated liquid water output at the base of the snowpack in (a) Rinertaelli and (b) Stillberg for the four model configurations.

The combination of the Richards equation and the scaling approaches results in improved performances in term of NSE coefficient and coefficient of determination (Table 2). Moreover, model results are much more accurate at Stillberg versus Rinertaelli, which can be partially explained by the proximity of the AWS station to the Stillberg site. These statistics also show that the precipitation interpolation method has a higher impact on model performance than the liquid water transport scheme.

5.3. Snowmelt Dynamics at the Basin Scale

At the basin scale, melt dynamics also change considerably for the different model configurations: this is illustrated by the temporal evolution

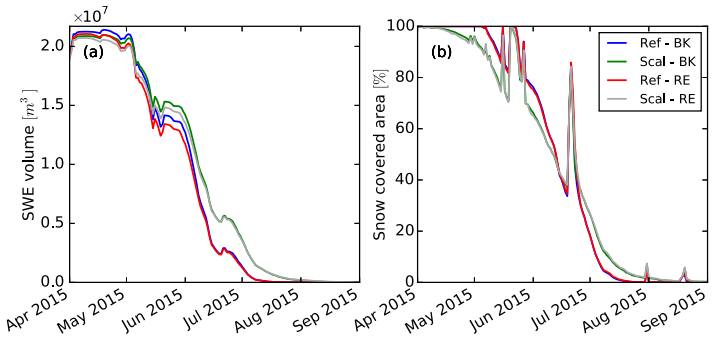

Figure 6. (a) Total SWE volume and (b) snow depletion curve (SDC) of the Dischma basin for the four model configurations. The spikes in the SDC correspond to snowfall events.

of total SWE and the snow depletion curves (SDC) over the Dischma basin (Figure 6). From mid-April to mid-May, the RE scheme generates slightly more liquid water output from the snowpack compared to the bucket scheme (Figure 6a). Afterward, the influence of the snow distribution becomes predominant: with increased snow heterogeneity, parts of the basin become snow free earlier, evident by the earlier decrease in snow-covered area (SCA) in the simulations using the scaling approach (Figure 6b). However, the scaling also leads to slower melt, and thus to larger SWE volumes and higher SCA values than in the reference case during the second half of the melting season. In late June, the difference between the two interpolation methods reaches up to 10% in SCA and more than 2.7 $\times$ 10^6 m^3 of SWE, doubling the remaining snow volume. The same dynamics are observed for the headwater catchment (not shown) with a difference in SCA of 20% and three times more SWE in early July.

The spatial patterns of snow distribution at peak accumulation obtained using the classic precipitation interpolation scheme (Figure 7a) show little heterogeneity (mean snow depth $HS_{Ref\text{-}BK} = 1.56$ m, standard deviation $\sigma_{Ref\text{-}BK} = 0.32$ m, compared to $HS_{obs} = 1.42$ m, $\sigma_{obs} = 0.71$ m). This spatial homogeneity is highlighted by the basin-wide histograms of snow depth at peak accumulation (supporting information Figure S2). Modeled variability for the reference scheme is principally controlled by the precipitation elevational gradient (supporting information Figure S3). The repeated melt events and rain-on-snow events that took place between October 2014 and January 2015 had little effect on the resulting snow heterogeneity and above statistics at peak accumulation (15 April 2017). Similarly, aspect variations across the basin did not play a dominant role in the resulting snow distribution during the accumulation season (supporting information Figure S4). Once the onset of spring melt sets in, a small increase in variability is observed ($\sigma_{Ref\text{-}BK} = 0.4$ m, supporting information Figure S2) as a result of the spatial variability of radiative fluxes induced by topography. Nevertheless, the initial snowpack heterogeneity is still the dominant control on the general dynamics of melt (supporting information Figure S2). This homogeneity is also clearly visible spatially: the symmetry is noticeable between the two main valley flanks (Figure 7b) while one would expect earlier snow melt on the southwest-facing slope. Finally, this uniformity leads to a shortening of the melting season because deeper accumulation areas are scarce (supporting information Figure S2).

With the scaling interpolation scheme, the heterogeneity of snow distribution (Figure 7 and supporting information Figure S2) throughout the melting season is enhanced since it includes effects of snow transport and early melt. The snow distribution at the onset of melt also agrees very well with the observations ($HS_{Scal\text{-}BK} = 1.55$ m, $\sigma_{Scal\text{-}BK} = 0.72$ m versus $HS_{obs} = 1.42$ m, $\sigma_{obs} = 0.71$ m). Snow accumulation as a function of elevation also differs significantly between the two precipitation interpolation methods, with lower accumulation below 2,300–2,400 m and a maximum between 2,500 and 2,600 m for the scaling interpolation scheme (supporting information Figure S3). There is a decrease in snow accumulation on southwest-facing slopes and an increase on all north-facing slopes (from northwest to northeast) with the scaling interpolation method (supporting information Figure S4). As observed at the site scale, the southeast-facing slopes of the Rinertaelli side-valley have a noticeably shallower snow accumulation. As the melt dynamics are strongly determined by the initial snowpack distribution, these features persist throughout the melt season (Figure 7 and supporting information Figure S2). Later, during the second half of the melt season, deeper snow accumulations remain on slopes close to ridges, while in the reference case, only shallow snow is present in these areas (compare maps c and g, d and h in Figure 7).

In the following paragraphs, we compare measured discharge at the outlet of two subbasins and the entire basin to cumulative soil runoff close to the surface (at 5 cm depth) integrated over each contributing area (Figure 8). This allows for a comparison between observations and modeling results without calibration. For the Rinertaelli subbasin, the total mass balance is almost independent of the chosen interpolation scheme but the snowpack distribution changes (Figure 8a and supporting information Figure S2). The heterogeneous snowpack leads to more melt water at the very beginning of the melt season, while later the reference configuration produces more runoff because the shallower snowpack portions in the scaling simulations have already disappeared and the remaining contributing area is smaller. On the other hand,

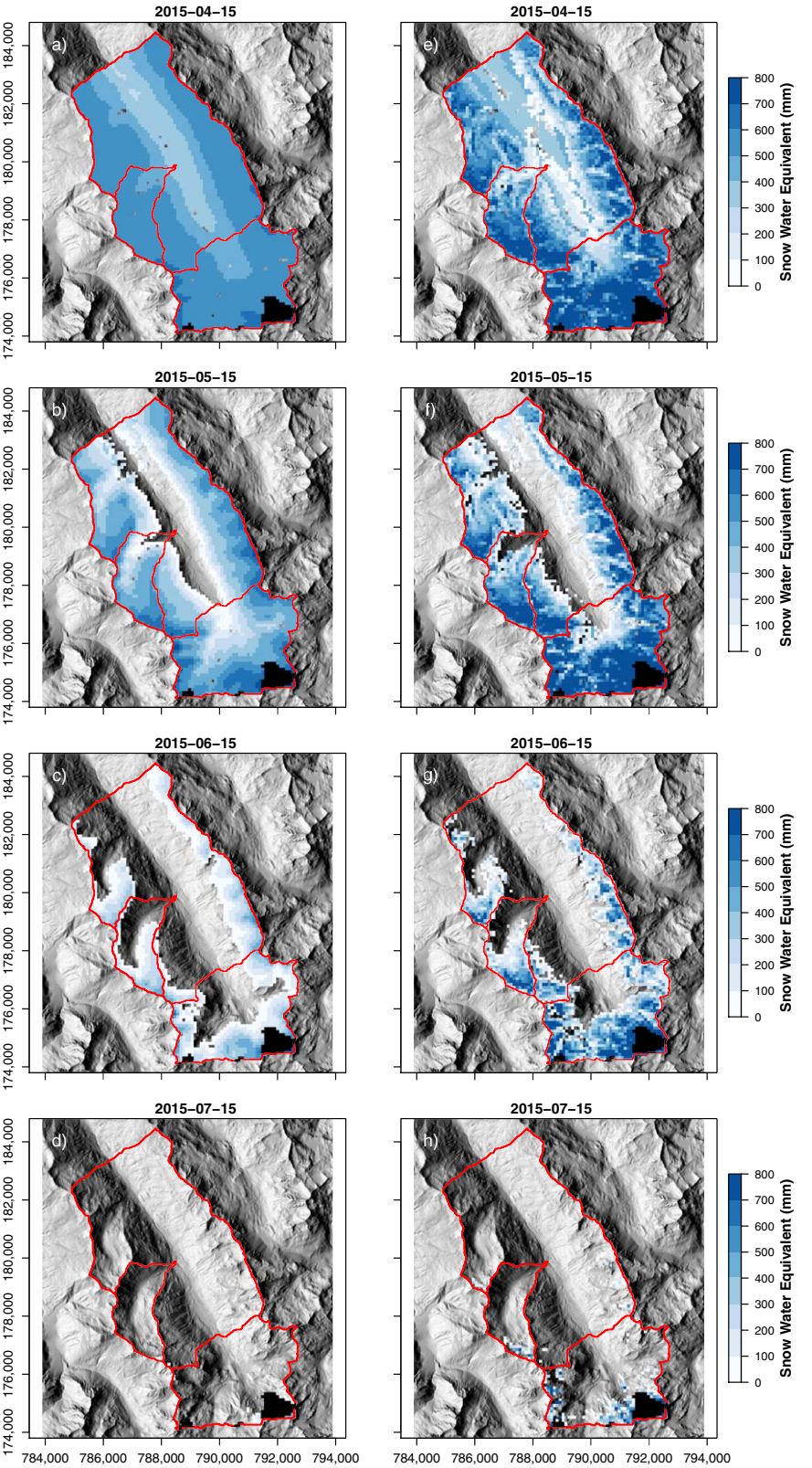

Figure 7. Comparison of the snow water equivalent (SWE) during the melting season for (a–d) the Ref-BK simulation and (e–h) the Scal-BK. The glacier is masked in black.

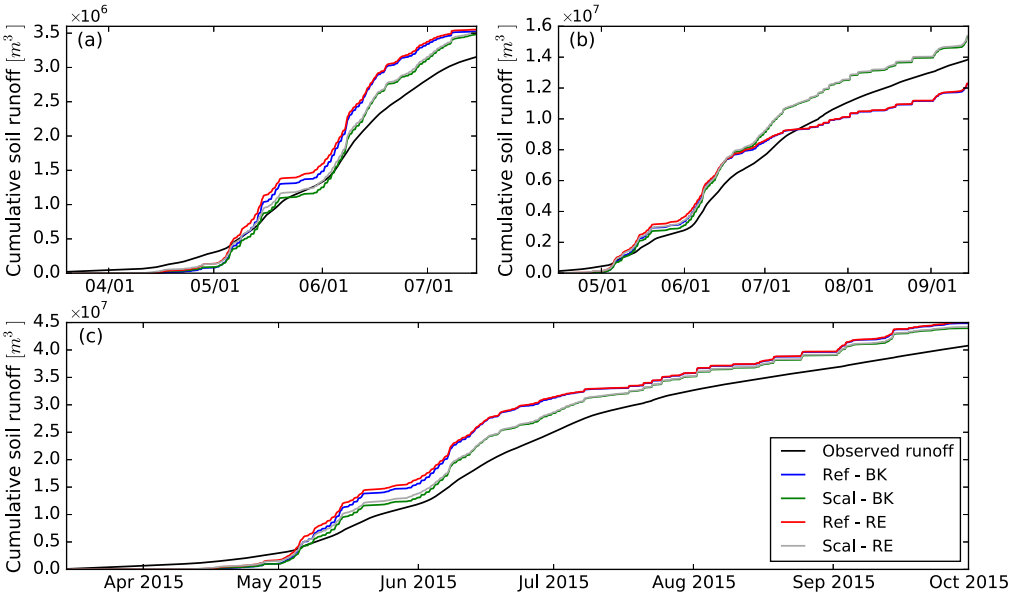

Figure 8. Comparison of cumulative soil infiltration runoff (at 5 cm depth) for the different model configurations and the observed discharge for (a) the Rinertaelli subbasin, (b) the Duerrboden subbasin, and (c) the entire Dischma basin.

the snowmelt season lasts longer due to deeper accumulations generated by the scaling approach. The water transport scheme changes the response only marginally due to averaging effects at the basin scale. Compared to the observed discharge, which starts earlier and has a larger magnitude, melt in April is consequently somewhat underestimated. This is coherent with the site-observations from the Rinertaelli, where the model underestimates the observed melt rate on south-facing slopes. In addition, the negative bias observed for shallow snow (0–0.5 m; Figure 2 and supporting information Figure S2) could also partly explain this underestimation.

In the Duerrboden catchment (Figure 8b), the influence of the snowpack spatial distribution on the soil runoff is even more evident than in the previous case since the mass balance is not conserved locally at the subbasin scale as the reference interpolation largely underestimates snow accumulations on the upper part of the basin (supporting information Figure S2). At the end of June, the simulations are diverging with snowmelt runoff remaining considerably lower in the reference simulations. Relative to the observations, this underestimation is clear; the soil runoff cannot sustain the measured runoff. Physically this would be possible if significant groundwater storage volume was available, however this is not the case in the upper Dischma basin.

By definition, the scaling method conserves mass over the entire Dischma catchment (Figure 8c). The results for the whole basin are partly similar to the ones observed previously, i.e., the hydrological response is mainly driven by the snow distribution (in contrast to the liquid water transport scheme). The scaling method slightly changes the beginning of the melt season (by 2–3 days) but most importantly extends its duration by more than a month. Compared to observations, the start of the melt season is heavily delayed (by more than 15 days). This last feature has already been observed when using *Alpine3D* for snow simulations of alpine catchments (e.g., Gallice et al., 2016; Lehning et al., 2006).

5.4. Hydrological Response

In the Rinertaelli basin, the general runoff pattern is fairly well represented by all configurations (Figure 9a) and model performances expressed as NSE coefficient are very similar (Table 3). However, some interesting features can be pointed out. First, the model fails to capture the timing of the onset of the melt season, with the first melt pulse occurring 30 days later than in the observations resulting in a strong underestimation of the discharge during that time. In May and June, the general streamflow dynamics are well captured but the magnitude is underestimated. On the contrary, from end of June, the discharge is overestimated in the four scenarios, which could be a direct consequence of the previously observed runoff underestimation

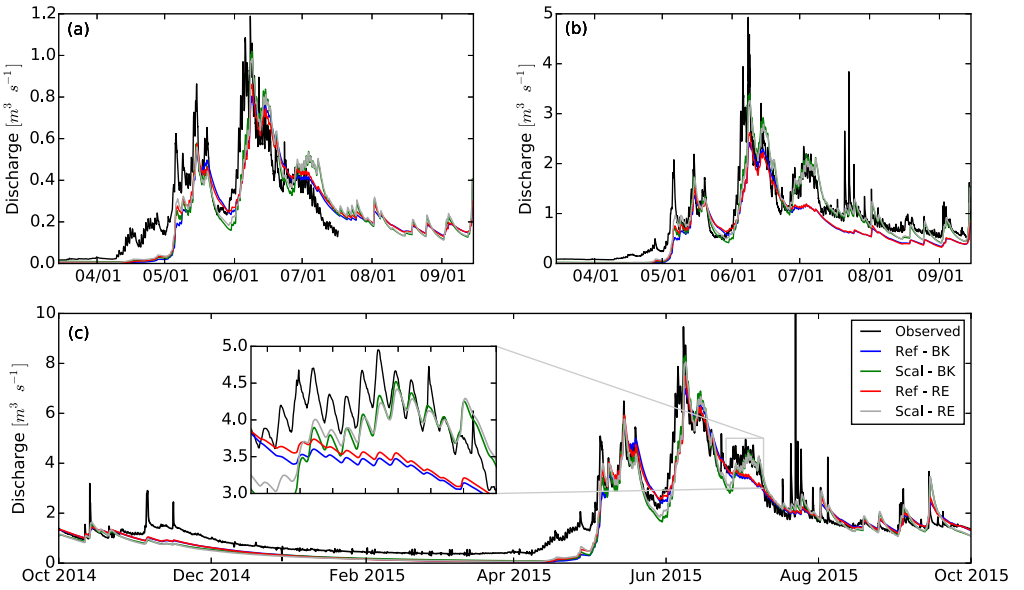

Figure 9. Observed and modeled discharge for (a) the Rinertaelli subbasin, (b) the Duerrboden subbasin, and (c) the entire Dischma basin. Note the different discharge scales between the three panels.

(from April to June). Even if these results are consistent with the ones at the site scale (underestimated melt intensities on south-facing slope, section 5.2) and subbasin scale (delayed onset of the melt season, section 5.3), the underestimation at the beginning of the snowmelt season at the subbasin scale is fairly large.

In the Duerrboden catchment, a more realistic snowpack significantly improves the hydrological simulation (NSE of 0.86 and 0.85 compared to 0.72 and 0.74, Table 3) mainly by correctly simulating the snowmelt season, which is longer by more than a month (see the change of the centroid in time [CT], a seasonality indicator (Stewart et al., 2005), in Table 3 and Figure 9b). In the reference configuration, the basin becomes snow free too early in the season, which results in a strong underestimation of the observed discharge from early July to October explaining the bad performance in terms of log NSE (Table 3). As already discussed for the soil runoff, differences between the two liquid water transport schemes are very small. Finally, the discharge underestimation in late April and May is visible in all simulations. This appears to be a model error possibly from the meteorological interpolation or from misrepresentation of subgrid processes, which is further addressed below in section 6.

Table 3
Performances of the Hydrological Model for the Three Monitored Basins in Terms of Nash-Sutcliffe Efficiency (NSE), log NSE Based on the Logarithmic Discharge Values and the Centroid in Time (CT) of the Daily Discharge (in Days Since 1 October)

		NSE	log NSE	CT (days)
Rinertaelli basin	Ref-BK	0.78	0.32	239.1
	Scal-BK	0.79	0.61	241.4
	Ref-RE	0.81	0.44	239.4
	Scal-RE	0.79	0.61	243.1
Duerrboden basin	Ref-BK	0.72	−0.97	244.4
	Scal-BK	0.86	0.27	248.0
	Ref-RE	0.74	−0.75	244.1
	Scal-RE	0.85	0.02	249.6
Dischma basin	Ref-BK	0.85	−0.38	235.2
	Scal-BK	0.86	0.05	237.8
	Ref-RE	0.87	−0.28	235.1
	Scal-RE	0.86	−0.13	239.2

At the Dischma outlet, model performance is high for all configurations with NSE coefficients between 0.85 and 0.87 (Table 3). Even though the basin size causes a noticeable smoothing of the discharge signal (Figure 9c), interesting lessons can be learned. An initial snowpack closer to observations improves the simulated discharge evolution, notably during the second half of the melt season when large snow accumulations sustain the discharge (see inset in Figure 9c and change in CT in Table 3). With the reference interpolation, the hydrological model compensates the lack of snow (in July and August) by an increase of the maximum recharge rate R_{max}. This leads to an intensive use of the lower reservoir, which has a longer residence time than the upper one and thus, the large bias observed in the headwater catchment is not visible anymore. This is one of the main drawbacks of model calibration: it will hide model underperformance by compensating through other mechanisms.

6. Discussion

The present study highlights the importance of having different types of observational data when trying to understand snowmelt variability

in a small alpine catchment. These data allow for a detailed and independent validation of different components in physically based and spatially distributed snow models such as *Alpine3D*, highlighting strengths and weaknesses of such type of models. At the same time, it is essential that observations also cover various spatial scales. Our results show how discharge data at subbasin scales highlight features that would have been missed with only one streamflow time series at the basin outlet (i.e., snowmelt sustaining the discharge in summer). This is because the discharge signals of the various subbasins are averaged out over aggregated scales. Finally, novel snow surveying techniques allow for improvements in snow modeling that were previously unavailable. Here we show how the assimilation of a distributed snow depth data set at resolutions of the order of 100 m for precipitation interpolation and validation of model results allows a better understanding of the hydrological system itself. Such assimilation also allows the identification of model deficiencies that are difficult to assess with traditional snow surveying techniques (e.g., manual snow depth surveys).

SNOWPACK was originally developed to model the one-dimensional snowpack evolution at the location of an *IMIS* weather station (Lehning et al., 1999). Consequently, good model performance at the site scale is not a surprise. However, the spatial interpolation of meteorological variables in complex terrain remains challenging and spatially distributed simulations are thus not trivial. The method of Vögeli et al. (2016) partially reduces the precipitation interpolation error. This change of the local mass balance translates in a change of the energy balance by reducing or increasing the thermal inertia of the snowpack (proportional to its mass). Moreover, the insulating effect of the snow and the presence (or absence) of a high albedo surface significantly modify the local energy budget. The combination of mass redistribution with the correct local components of the energy balance improves the results considerably (for example NSE = 0.23 versus NSE = −1.36 in Rinertaelli). As for the liquid water transport, the gains in term of performance are less significant between the two schemes, i.e., the bucket and Richards equation methods. However, the Richards equation approach leads to improvements in the representation of the snowmelt output dynamics at the base of the snowpack when compared to hourly observations at the point scale, confirming earlier studies at extensively instrumented sites (Wever et al., 2014, 2015). The present study had to rely on interpolated meteorological data only. At the Rinertaelli site, the beginning of the melt period and its diurnal cycle are well captured. Modeled liquid output intensities are nevertheless lower than observed. Given that the second lysimeter (located close to a AWS) is very well simulated (NSE = 0.59), we would suspect an error of shortwave and/or longwave radiation interpolation or that the interpolation scheme misses local temperature and wind maxima induced by micrometeorological phenomenon. Even if we cannot completely exclude a measurement error of the lysimeter, the large discharge underestimation observed in the Rinertaelli subbasin is therefore not fully explained. Unfortunately, we have no meteorological observation to validate our hypothesis.

As shown by Anderton et al. (2004), seasonal snowmelt dynamics at subcatchment scales are mainly driven by the snowpack distribution at the peak of accumulation. Then the challenge is to get a realistic snowpack distribution as an initial stage variable for snowmelt modeling, even in a well-instrumented area. As observed here and in several previous studies (Grünewald et al., 2014; Grünewald & Lehning, 2011; Jonas et al., 2009; Sevruk, 1997), precipitation and SWE exhibit a positive trend with elevation. However, considering only a linear altitudinal gradient leads to a too simplistic snow distribution. In reality, several processes such as preferential deposition, snow transport by winds, and avalanching lead to larger heterogeneity (Clark et al., 2011). In this study, we applied the approach by Vögeli et al. (2016) for precipitation interpolation and mass accumulation. It has the merit of being computationally efficient and provides an initial snowpack distribution closer to the observations. The methodology also implicitly corrects for some of the processes mentioned above that are difficult to model explicitly, e.g., precipitation preferential deposition, snow transport, and avalanching. However, this approach requires a meticulous analysis of the ADS snow distribution to identify potential biases (e.g., heterogeneous snowmelt before date of flight) that could be introduced directly into the model results. In our case, due to the relatively large elevation gradient in the basin, the data set has a small negative bias for shallow snow and low elevations due to limited melt. This could be a second partial explanation of the underestimation observed in the discharge time series at the beginning of the melt season. Finally, the scaling method implicitly assumes that peak snow accumulation occurs simultaneously over the entire basin. Even if this classic categorization into an accumulation and an ablation season is convenient, this assumption is mainly but not fully fulfilled in our high-alpine case study.

This condition is certainly not valid in regions with larger elevation and climatic gradients and, in general, will be less and less the case due to climate change in higher elevations. Thus, the scaling method must be applied cautiously. In a warmer climate, the significance of spatial snow variability for mountain hydrology will be fundamental, notably in terms of timing. As shown in our results, large snow accumulations are strongly underestimated by a traditional interpolation scheme. This snow storage is essential to extend the duration of the melt season and sustain the observed discharge in summer. These considerations tend toward the development of more physical/dynamic methods to model the spatial variability of snow.

We intentionally chose the *StreamFlow* model because of its limited number of parameters, as the objective was to study the influence of snowpack differences rather than the calibration capacity of the model. Unfortunately, the calibrated hydrological model acts as a low-pass filter on input signals and smoothens a large portion of the differences. However, we showed that the vertical snowpack liquid water transport scheme has a limited impact on the hydrological response at the catchment scale. Conversely, the snow distribution has a significant influence on the discharge at the subbasin scale (Table 3) and for the whole catchment (*getting the right answer for the right reasons*). With a more realistic snowpack distribution, the melt season starts earlier and lasts longer, more coherent with observations. These results are also in agreement with previous studies (Luce et al., 1998; Warscher et al., 2013; Winstral et al., 2013) for which snow transport was considered. If we focus our attention on model performance (Table 3), differences are relatively small, which raises the question whether the increasing complexity is worth the small added value. In our opinion, simpler models can still be a good choice for many (operational) applications while physically based models would be more appropriate when trying to understand detailed snow and hydrological processes.

One of the results from our study is that the beginning of the melt season is not captured accurately whatever configuration of *Alpine3D* is chosen. The significance of the discrepancy indicates a misrepresentation or a missing process in the model. In reality, snow processes are taking place at varying spatial and temporal scales (Blöschl, 1999). In our case, the spatial resolution seems adequate to reproduce the large-scale features (regional and watershed scales). Nevertheless, we certainly miss some subgrid processes that take place at hillslope and local scales. For example, at the beginning of the melt season, the snowpack can be patchy due to the presence of boulders or rock faces exposed to the sun. Such situation can lead to an albedo feedback or modify the surrounding radiative budget enhancing melt. Recent work in the same region has also pointed out a strong feedback of the snow patch distribution on the local (katabatic/anabatic) wind and temperature fields (Mott et al., 2015). At the beginning of the melt season (high SCA), these circulation processes lead to an increase of the sensible heat flux toward the snowpack and then an intensification of ablation processes. As diurnal mountain winds are thermally driven, they particularly take place on south-facing slopes, but cannot be modeled in the present version of *Alpine3D* as no lateral exchange between grid elements is considered or would require the coupling of an atmospheric model (e.g., *ARPS* or *WRF*). Once the ablation season started, the lateral meltwater transport at the snow/soil interface (Eiriksson et al., 2013) and more generally the overland flow could also accelerate the hydrological response by bypassing the soil compartment. When the meltwater infiltrates into the soil, it displaces old water (known as translatory flow; DeWalle & Rango, 2008) and can rapidly generate runoff in the stream. All these elements support a proper integration of subgrid variability in snow models.

7. Conclusions

In this study, we analyze the effects of snow accumulation patterns and liquid water transport within the snowpack on snowmelt dynamics and on the hydrological response of an alpine catchment in the Swiss Alps. Our analyses combine in situ measurements of subhourly snowmelt output on north-facing and south-facing slopes, streamflow at the outlet of two small tributaries and at the outlet of the entire catchment, distributed snow depths from airborne photogrammetry, and output from the *Alpine3D* spatially distributed snow model for the water year 2014–2015.

During the accumulation period, we show how a novel precipitation scaling approach for spatial interpolation leads to an improvement in the estimation of snow distribution at peak accumulation when compared to a more traditional interpolation method ($R^2 = 0.96$ versus $R^2 = 0.34$). The simulated spatial pattern of peak accumulation differs by only 0.27 m in terms of RMSE when compared to measured snow depths at the 100 m scale. These results highlight the relevance of precipitation interpolation schemes for accurate

representation of peak snow accumulation and distribution even in a well-instrumented area. Furthermore, we show how accurate representation of snow distribution at peak accumulation is key for accurate representation of snowmelt processes and differential melt. Simulated results demonstrate that the increased heterogeneity of snow accumulation obtained using the scaling interpolation approach produces differential melt patterns with rapid melt from shallower snow accumulation areas, due to reduced thermal inertia and melt water travel time in the snowpack, compared to slower melt from areas of deeper snow located at high elevation. These differential patterns translate in faster runoff generation at the onset of the melting season from shallower snow packs and a prolonged snowmelt season duration because of the delayed melt from the deeper snow accumulation areas. Such differential melt patterns and runoff responses are severely muted when the more traditional precipitation interpolation method is used. Finally, we show that improvements in the representation of the spatial variability of snow lead to an improvement of the NSE by up to 0.12 for the simulated streamflow when compared to measurements at two different locations, within the basin and at the outlet.

Simulations using a Richards equation scheme allow for faster drainage of liquid water toward the base of the snowpack when compared to the standard bucket approach that was originally implemented in the *SNOWPACK* model. The effect of these improvements is reflected in a more realistic liquid water output from the snowpack in terms of timing and daily cycle at the site scale. At larger scales, the impact of the liquid water transport scheme is rather limited.

Acknowledgments
We thank Aurélien Gallice for his help in the field. ADS flights have been sponsored by Leica Geosystems. ADS flight processing has been done with the help of Yves Bühler and Mauro Marty. Part of the work and measurement infrastructure has been supported by the Swiss National Science Foundation project "Snow-atmosphere interactions driving snow accumulation and ablation in an Alpine catchment" (200021_150146). The models used here are available at http://models.slf.ch/. All results are available on the Envidat platform (www.envidat.ch) under https://doi.org/10.16904/envidat.24. Data from *Meteoswiss* (meteoswiss.admin.ch), *IMIS network* (www.slf.ch), *swisstopo* (swisstopo.admin.ch), and *FOEN* (hydrodaten.admin.ch) can be directly requested via the respective websites and are acknowledged.

References

Anderton, S. P., White, S. M., & Alvera, B. (2004). Evaluation of spatial variability in snow water equivalent for a high mountain catchment. *Hydrological Processes*, *18*(3), 435–453. https://doi.org/10.1002/hyp.1319

Aschwanden, H., Weingartner, R., & Geographie-Gewässerkunde, U. B. A. P. (1985). *Die Abflussregimes der Schweiz*. Bern, Switzerland: Geographisches Institut der Universität Bern, Abt. Physikalische Geographie-Gewässerkunde.

Bales, R. C., Hopmans, J. W., O'Geen, A. T., Meadows, M., Hartsough, P. C., Kirchner, P., . . . Beaudette, D. (2011). Soil moisture response to snowmelt and rainfall in a Sierra Nevada mixed-conifer forest. *Vadose Zone Journal*, *10*(3), 786. https://doi.org/10.2136/vzj2011.0001

Bales, R. C., Molotch, N. P., Painter, T. H., Dettinger, M. D., Rice, R., & Dozier, J. (2006). Mountain hydrology of the western United States. *Water Resources Research*, *42*, W08432. https://doi.org/10.1029/2005WR004387

Barnett, T. P., Adam, J. C., & Lettenmaier, D. P. (2005). Potential impacts of a warming climate on water availability in snow-dominated regions. *Nature*, *438*(7066), 303–309. https://doi.org/10.1038/nature04141

Bavay, M., & Egger, T. (2014). MeteoIO 2.4.2: A preprocessing library for meteorological data. *Geoscientific Model Development*, *7*(6), 3135–3151. https://doi.org/10.5194/gmd-7-3135-2014

Bavay, M., Grünewald, T., & Lehning, M. (2013). Response of snow cover and runoff to climate change in high Alpine catchments of Eastern Switzerland. *Advances in Water Resources*, *55*, 4–16. https://doi.org/10.1016/j.advwatres.2012.12.009

Bavay, M., Lehning, M., Jonas, T., & Löwe, H. (2009). Simulations of future snow cover and discharge in Alpine headwater catchments. *Hydrological Processes*, *23*(1), 95–108. https://doi.org/10.1002/hyp.7195

Beniston, M. (1997). Variations of snow depth and duration in the Swiss Alps over the last 50 years: Links to changes in large-scale climatic forcings. In H. F. Diaz, M. Beniston, & R. S. Bradley (Eds.), *Climatic change at high elevation sites* (pp. 49–68). Dordrecht, the Netherlands: Springer. https://doi.org/10.1007/978-94-015-8905-5_3

Blöschl, G. (1999). Scaling issues in snow hydrology. *Hydrological Processes*, *13*(14–15), 2149–2175. https://doi.org/10.1002/(SICI)1099-1085(199910)13:14/15 < 2149::AID-HYP847 > 3.0.CO;2–8

Blöschl, G., & Kirnbauer, R. (1992). An analysis of snow cover patterns in a small alpine catchment. *Hydrological Processes*, *6*(1), 99–109. https://doi.org/10.1002/hyp.3360060109

Botter, G., Bertuzzo, E., & Rinaldo, A. (2010). Transport in the hydrologic response: Travel time distributions, soil moisture dynamics, and the old water paradox. *Water Resources Research*, *46*, W03514. https://doi.org/10.1029/2009WR008371

Brun, E., Martin, E., Simon, V., Gendre, C., & Coleou, C. (1989). An energy and mass model of snow cover suitable for operational avalanche forecasting. *Journal of Glaciology*, *35*(121), 333–342. https://doi.org/10.3198/1989JoG35-121-333-342

Bühler, Y., Marty, M., Egli, L., Veitinger, J., Jonas, T., Thee, P., & Ginzler, C. (2015). Snow depth mapping in high-alpine catchments using digital photogrammetry. *The Cryosphere*, *9*(1), 229–243. https://doi.org/10.5194/tc-9-229-2015

Burn, D. H. (1994). Hydrologic effects of climatic change in west-central Canada. *Journal of Hydrology*, *160*(1–4), 53–70. https://doi.org/10.1016/0022-1694(94)90033-7

Clark, M. P., Hendrikx, J., Slater, A. G., Kavetski, D., Anderson, B., Cullen, N. J., . . . Woods, R. A. (2011). Representing spatial variability of snow water equivalent in hydrologic and land-surface models: A review. *Water Resources Research*, *47*, W07539. https://doi.org/10.1029/2011WR010745

Comola, F., Schaefli, B., Rinaldo, A., & Lehning, M. (2015). Thermodynamics in the hydrologic response: Travel time formulation and application to Alpine catchments. *Water Resources Research*, *51*, 1671–1687. https://doi.org/10.1002/2014WR016228

Comola, F., Schaefli, B., Ronco, P. D., Botter, G., Bavay, M., Rinaldo, A., & Lehning, M. (2015). Scale-dependent effects of solar radiation patterns on the snow-dominated hydrologic response. *Geophysical Research Letters*, *42*, 3895–3902. https://doi.org/10.1002/2015GL064075

Day, T. J. (1976). On the precision of salt dilution gauging. *Journal of Hydrology*, *31*(3), 293–306. https://doi.org/10.1016/0022-1694(76)90130-X

DeWalle, D. R., & Rango, A. (2008). *Principles of snow hydrology*. Cambridge, UK: Cambridge University Press.

Dozier, J. (2011). Mountain hydrology, snow color, and the fourth paradigm. *Eos, Transactions American Geophysical Union*, *92*(43), 373–374. https://doi.org/10.1029/2011EO430001

Eiriksson, D., Whitson, M., Luce, C. H., Marshall, H. P., Bradford, J., Benner, S. G., . . . McNamara, J. P. (2013). An evaluation of the hydrologic relevance of lateral flow in snow at hillslope and catchment scales. *Hydrological Processes*, *27*(5), 640–654. https://doi.org/10.1002/hyp.9666

Essery, R., Rutter, N., Pomeroy, J., Baxter, R., Stähli, M., Gustafsson, D., . . . Elder, K. (2009). SNOWMIP2: An evaluation of forest snow process simulations. *Bulletin of the American Meteorological Society*, *90*(8), 1120–1135. https://doi.org/10.1175/2009BAMS2629.1

Etchevers, P., Martin, E., Brown, R., Fierz, C., Lejeune, Y., Bazile, E., . . . Yang, Z.-L. (2004). Validation of the energy budget of an alpine snowpack simulated by several snow models (SnowMIP project). *Annals of Glaciology*, *38*(1), 150–158. https://doi.org/10.3189/172756404781814825

FOEN. (2017). *Federal Office for the Environment-Hydrological data and forecasts*. Retrieved from http://www.hydrodaten.admin.ch/en/2327.html

Frei, C., & Schär, C. (1998). A precipitation climatology of the Alps from high-resolution rain-gauge observations. *International Journal of Climatology*, *18*(8), 873–900. https://doi.org/10.1002/(SICI)1097-0088(19980630)18:8<873::AID-JOC255>3.0.CO;2–9

Gallice, A., Bavay, M., Brauchli, T., Comola, F., Lehning, M., & Huwald, H. (2016). StreamFlow 1.0: An extension to the spatially distributed snow model Alpine3D for hydrological modelling and deterministic stream temperature prediction. *Geoscientific Model Development*, *9*(12), 4491–4519. https://doi.org/10.5194/gmd-9-4491-2016

Goodison, B. E., Louie, P. Y. T., & Yang, D. (1997). *The WMO solid precipitation measurement intercomparison* (World Meteorol. Org. Publ. WMO TD, pp. 65–70).

Gouttevin, I., Lehning, M., Jonas, T., Gustafsson, D., & Mölder, M. (2015). A two-layer canopy model with thermal inertia for an improved snowpack energy balance below needleleaf forest (model SNOWPACK, version 3.2.1, revision 741). *Geoscientific Model Development*, *8*(8), 2379–2398. https://doi.org/10.5194/gmd-8-2379-2015

Grünewald, T., Bühler, Y., & Lehning, M. (2014). Elevation dependency of mountain snow depth. *The Cryosphere*, *8*(6), 2381–2394. https://doi.org/10.5194/tc-8-2381-2014

Grünewald, T., & Lehning, M. (2011). Altitudinal dependency of snow amounts in two small alpine catchments: Can catchment-wide snow amounts be estimated via single snow or precipitation stations? *Annals of Glaciology*, *52*(58), 153–158. https://doi.org/10.3189/172756411797252248

Grünewald, T., Schirmer, M., Mott, R., & Lehning, M. (2010). Spatial and temporal variability of snow depth and ablation rates in a small mountain catchment. *The Cryosphere*, *4*(2), 215–225. https://doi.org/10.5194/tc-4-215-2010

Gurtz, J., Zappa, M., Jasper, K., Lang, H., Verbunt, M., Badoux, A., & Vitvar, T. (2003). A comparative study in modelling runoff and its components in two mountainous catchments. *Hydrological Processes*, *17*(2), 297–311. https://doi.org/10.1002/hyp.1125

Harding, R. J., & Pomeroy, J. W. (1996). The energy balance of the winter boreal landscape. *Journal of Climate*, *9*(11), 2778–2787. https://doi.org/10.1175/1520-0442(1996)009<2778:TEBOTW>2.0.CO;2

Horton, P., Schaefli, B., Mezghani, A., Hingray, B., & Musy, A. (2006). Assessment of climate-change impacts on alpine discharge regimes with climate model uncertainty. *Hydrological Processes*, *20*(10), 2091–2109. https://doi.org/10.1002/hyp.6197

Jonas, T., Marty, C., & Magnusson, J. (2009). Estimating the snow water equivalent from snow depth measurements in the Swiss Alps. *Journal of Hydrology*, *378*(1–2), 161–167. https://doi.org/10.1016/j.jhydrol.2009.09.021

Kattelmann, R. (2000). Snowmelt lysimeters in the evaluation of snowmelt models. *Annals of Glaciology*, *31*(1), 406–410. https://doi.org/10.3189/172756400781820048

Kinar, N. J., & Pomeroy, J. W. (2015). Measurement of the physical properties of the snowpack. *Reviews of Geophysics*, *53*, 481–544. https://doi.org/10.1002/2015RG000481

Lehning, M. (2006). Energy balance and thermophysical processes in snowpacks. In *Encyclopedia of hydrological sciences*. Hoboken, NJ: John Wiley.

Lehning, M., Bartelt, P., Brown, B., Russi, T., Stöckli, U., & Zimmerli, M. (1999). Snowpack model calculations for avalanche warning based upon a new network of weather and snow stations. *Cold Regions Science and Technology*, *30*(1–3), 145–157. https://doi.org/10.1016/S0165-232X(99)00022-1

Lehning, M., Löwe, H., Ryser, M., & Raderschall, N. (2008). Inhomogeneous precipitation distribution and snow transport in steep terrain. *Water Resources Research*, *44*, W07404. https://doi.org/10.1029/2007WR006545

Lehning, M., Völksch, I., Gustafsson, D., Nguyen, T. A., Stähli, M., & Zappa, M. (2006). ALPINE3D: A detailed model of mountain surface processes and its application to snow hydrology. *Hydrological Processes*, *20*(10), 2111–2128. https://doi.org/10.1002/hyp.6204

Luce, C. H., Tarboton, D. G., & Cooley, K. R. (1998). The influence of the spatial distribution of snow on basin-averaged snowmelt. *Hydrological Processes*, *12*(10–11), 1671–1683. https://doi.org/10.1002/(SICI)1099-1085(199808/09)12:10/11<1671::AID-HYP688>3.0.CO;2-N

Lundquist, J. D., & Dettinger, M. D. (2005). How snowpack heterogeneity affects diurnal streamflow timing. *Water Resources Research*, *41*, W05007. https://doi.org/10.1029/2004WR003649

Marks, D., Domingo, J., Susong, D., Link, T., & Garen, D. (1999). A spatially distributed energy balance snowmelt model for application in mountain basins. *Hydrological Processes*, *13*(12–13), 1935–1959. https://doi.org/10.1002/(SICI)1099-1085(199909)13:12/13<1935::AID-HYP868>3.0.CO;2-C

Marks, D., & Dozier, J. (1992). Climate and energy exchange at the snow surface in the Alpine Region of the Sierra Nevada: 2. Snow cover energy balance. *Water Resources Research*, *28*(11), 3043–3054. https://doi.org/10.1029/92WR01483

Marty, C., Schlögl, S., Bavay, M., & Lehning, M. (2017). How much can we save? Impact of different emission scenarios on future snow cover in the Alps. *The Cryosphere*, *11*(1), 517–529. https://doi.org/10.5194/tc-11-517-2017

Menzel, L., Lang, H., & Rohmann, M. (1999). Plate 4.1 mean annual actual evaporation 1973–1992. In *Hydrological Atlas of Switzerland*. Bern, Switzerland: Universität Bern.

Michlmayr, G., Lehning, M., Koboltschnig, G., Holzmann, H., Zappa, M., Mott, R., & Schöner, W. (2008). Application of the Alpine 3D model for glacier mass balance and glacier runoff studies at Goldbergkees, Austria. *Hydrological Processes*, *22*(19), 3941–3949. https://doi.org/10.1002/hyp.7102

Mott, R., Daniels, M., & Lehning, M. (2015). Atmospheric flow development and associated changes in turbulent sensible heat flux over a patchy mountain snow cover. *Journal of Hydrometeorology*, *16*(3), 1315–1340. https://doi.org/10.1175/JHM-D-14-0036.1

Mott, R., Gromke, C., Grünewald, T., & Lehning, M. (2013). Relative importance of advective heat transport and boundary layer decoupling in the melt dynamics of a patchy snow cover. *Advances in Water Resources*, *55*, 88–97. https://doi.org/10.1016/j.advwatres.2012.03.001

Mott, R., & Lehning, M. (2010). Meteorological modeling of very high-resolution wind fields and snow deposition for mountains. *Journal of Hydrometeorology*, *11*(4), 934–949. https://doi.org/10.1175/2010JHM1216.1

Mott, R., Schirmer, M., Bavay, M., Grünewald, T., & Lehning, M. (2010). Understanding snow-transport processes shaping the mountain snow-cover. *The Cryosphere*, *4*(4), 545–559. https://doi.org/10.5194/tc-4-545-2010

Mott, R., Scipión, D., Schneebeli, M., Dawes, N., Berne, A., & Lehning, M. (2014). Orographic effects on snow deposition patterns in mountainous terrain. *Journal of Geophysical Research: Atmospheres*, *119*, 1419–1439. https://doi.org/10.1002/2013JD019880

Musselman, K. N., Clark, M. P., Liu, C., Ikeda, K., & Rasmussen, R. (2017). Slower snowmelt in a warmer world. *Nature Climate Change*, *7*(3), 214–219. https://doi.org/10.1038/nclimate3225

Nash, J. E., & Sutcliffe, J. V. (1970). River flow forecasting through conceptual models part I—A discussion of principles. *Journal of Hydrology*, *10*(3), 282–290. https://doi.org/10.1016/0022-1694(70)90255-6

Roe, G. H. (2005). Orographic precipitation. *Annual Review of Earth and Planetary Sciences*, *33*(1), 645–671. https://doi.org/10.1146/annurev.earth.33.092203.122541

Schädler, B., & Weingartner, R. (1992). Plate 5.4 natural runoff 1961–1980. In *Hydrological Atlas of Switzerland*. Bern, Switzerland: Universität Bern.

Schaefli, B., Hingray, B., & Musy, A. (2007). Climate change and hydropower production in the Swiss Alps: Quantification of potential impacts and related modelling uncertainties. *Hydrology and Earth System Sciences*, *11*(3), 1191–1205. https://doi.org/10.5194/hess-11-1191-2007

Schirmer, M., Wirz, V., Clifton, A., & Lehning, M. (2011). Persistence in intra-annual snow depth distribution: 1. Measurements and topographic control. *Water Resources Research*, *47*, W09516. https://doi.org/10.1029/2010WR009426

Schlögl, S., Marty, C., Bavay, M., & Lehning, M. (2016). Sensitivity of Alpine3D modeled snow cover to modifications in DEM resolution, station coverage and meteorological input quantities. *Environmental Modelling & Software*, *83*, 387–396. https://doi.org/10.1016/j.envsoft.2016.02.017

Schmucki, E., Marty, C., Fierz, C., & Lehning, M. (2014). Evaluation of modelled snow depth and snow water equivalent at three contrasting sites in Switzerland using SNOWPACK simulations driven by different meteorological data input. *Cold Regions Science and Technology*, *99*, 27–37. https://doi.org/10.1016/j.coldregions.2013.12.004

Schmucki, E., Marty, C., Fierz, C., Weingartner, R., & Lehning, M. (2017). Impact of climate change in Switzerland on socioeconomic snow indices. *Theoretical and Applied Climatology*, *127*(3–4), 875–889. https://doi.org/10.1007/s00704-015-1676-7

Scipión, D. E., Mott, R., Lehning, M., Schneebeli, M., & Berne, A. (2013). Seasonal small-scale spatial variability in alpine snowfall and snow accumulation. *Water Resources Research*, *49*, 1446–1457. https://doi.org/10.1002/wrcr.20135

Scott, D., Dawson, J., & Jones, B. (2008). Climate change vulnerability of the US Northeast winter recreation—Tourism sector. *Mitigation and Adaptation Strategies for Global Change*, *13*(5–6), 577–596. https://doi.org/10.1007/s11027-007-9136-z

Serreze, M. C., Clark, M. P., Armstrong, R. L., McGinnis, D. A., & Pulwarty, R. S. (1999). Characteristics of the western United States snowpack from snowpack telemetry (SNOTEL) data. *Water Resources Research*, *35*(7), 2145–2160. https://doi.org/10.1029/1999WR900090

Sevruk, B. (1997). Regional dependency of precipitation-altitude relationship in the Swiss Alps. In H. F. Diaz, M. Beniston, & R. S. Bradley (Eds.), *Climatic change at high elevation sites* (pp. 123–137). Dordrecht, the Netherlands: Springer.

Sommer, C. G., Lehning, M., & Mott, R. (2015). Snow in a very steep rock face: Accumulation and redistribution during and after a snowfall event. *Frontiers in Earth Science*, *3*, 73. https://doi.org/10.3389/feart.2015.00073

Spreafico, M., & Weingartner, R. (2005). *The hydrology of Switzerland. Selected aspects and results. Reports, Bundesamt Für Wasser Und Geologie (BWG) water series 7*. Bern, Switzerland: Federal Office for Water and Geology.

Stewart, I. T. (2009). Changes in snowpack and snowmelt runoff for key mountain regions. *Hydrological Processes*, *23*(1), 78–94. https://doi.org/10.1002/hyp.7128

Stewart, I. T., Cayan, D. R., & Dettinger, M. D. (2005). Changes toward earlier streamflow timing across Western North America. *Journal of Climate*, *18*(8), 1136–1155. https://doi.org/10.1175/JCLI3321.1

Tarboton, D. G. (1997). A new method for the determination of flow directions and upslope areas in grid digital elevation models. *Water Resources Research*, *33*(2), 309–319. https://doi.org/10.1029/96WR03137

Trujillo, E., Molotch, N. P., Goulden, M. L., Kelly, A. E., & Bales, R. C. (2012). Elevation-dependent influence of snow accumulation on forest greening. *Nature Geoscience*, *5*(10), 705–709. https://doi.org/10.1038/ngeo1571

Trujillo, E., Ramírez, J. A., & Elder, K. J. (2007). Topographic, meteorologic, and canopy controls on the scaling characteristics of the spatial distribution of snow depth fields. *Water Resources Research*, *43*, W07409. https://doi.org/10.1029/2006WR005317

Trujillo, E., Ramírez, J. A., & Elder, K. J. (2009). Scaling properties and spatial organization of snow depth fields in sub-alpine forest and alpine tundra. *Hydrological Processes*, *23*(11), 1575–1590. https://doi.org/10.1002/hyp.7270

Van Genuchten, M. T. (1980). A closed-form equation for predicting the hydraulic conductivity of unsaturated soils. *Soil Science Society of America Journal*, *44*(5), 892–898.

Verbunt, M., Gurtz, J., Jasper, K., Lang, H., Warmerdam, P., & Zappa, M. (2003). The hydrological role of snow and glaciers in alpine river basins and their distributed modeling. *Journal of Hydrology*, *282*(1–4), 36–55. https://doi.org/10.1016/S0022-1694(03)00251-8

Viviroli, D., Archer, D. R., Buytaert, W., Fowler, H. J., Greenwood, G. B., Hamlet, A. F., . . . Woods, R. (2011). Climate change and mountain water resources: Overview and recommendations for research, management and policy. *Hydrology and Earth System Sciences*, *15*(2), 471–504. https://doi.org/10.5194/hess-15-471-2011

Vögeli, C., Lehning, M., Wever, N., & Bavay, M. (2016). Scaling precipitation input to spatially distributed hydrological models by measured snow distribution. *Frontiers in Earth Science*, *4*, 108. https://doi.org/10.3389/feart.2016.00108

Warscher, M., Strasser, U., Kraller, G., Marke, T., Franz, H., & Kunstmann, H. (2013). Performance of complex snow cover descriptions in a distributed hydrological model system: A case study for the high Alpine terrain of the Berchtesgaden Alps. *Water Resources Research*, *49*, 2619–2637. https://doi.org/10.1002/wrcr.20219

Weijs, S. V., Mutzner, R., & Parlange, M. B. (2013). Could electrical conductivity replace water level in rating curves for alpine streams? *Water Resources Research*, *49*, 343–351. https://doi.org/10.1029/2012WR012181

Westerling, A. L. (2006). Warming and earlier spring increase Western U.S. forest wildfire activity. *Science*, *313*(5789), 940–943. https://doi.org/10.1126/science.1128834

Wever, N., Comola, F., Bavay, M., & Lehning, M. (2017). Simulating the influence of snow surface processes on soil moisture dynamics and streamflow generation in an alpine catchment. *Hydrology and Earth System Sciences*, *21*(8), 4053–4071. https://doi.org/10.5194/hess-21-4053-2017

Wever, N., Fierz, C., Mitterer, C., Hirashima, H., & Lehning, M. (2014). Solving Richards Equation for snow improves snowpack meltwater runoff estimations in detailed multi-layer snowpack model. *The Cryosphere*, *8*(1), 257–274. https://doi.org/10.5194/tc-8-257-2014

Wever, N., Schmid, L., Heilig, A., Eisen, O., Fierz, C., & Lehning, M. (2015). Verification of the multi-layer SNOWPACK model with different water transport schemes. *The Cryosphere*, *9*(6), 2271–2293. https://doi.org/10.5194/tc-9-2271-2015

Winchell, T. S., Barnard, D. M., Monson, R. K., Burns, S. P., & Molotch, N. P. (2016). Earlier snowmelt reduces atmospheric carbon uptake in midlatitude subalpine forests. *Geophysical Research Letters*, *43*, 8160–8168. https://doi.org/10.1002/2016GL069769

Winstral, A., Marks, D., & Gurney, R. (2013). Simulating wind-affected snow accumulations at catchment to basin scales. *Advances in Water Resources*, *55*, 64–79. https://doi.org/10.1016/j.advwatres.2012.08.011

Woo, M.-K. (2006). Snowmelt runoff generation. In *Encyclopedia of hydrological sciences*. Hoboken, NJ: John Wiley.

Würzer, S., Wever, N., Juras, R., Lehning, M., & Jonas, T. (2016). Modeling liquid water transport in snow under rain-on-snow conditions—Considering preferential flow. *Hydrology and Earth System Sciences Discussions*, *21*, 1741–1756. https://doi.org/10.5194/hess-2016-351

Yamaguchi, S., Watanabe, K., Katsushima, T., Sato, A., & Kumakura, T. (2012). Dependence of the water retention curve of snow on snow characteristics. *Annals of Glaciology*, *53*(61), 6–12.